CHANGES IN ADHESION OF CrN COATINGS ON Zr-1%Nb ALLOY SUBSTRATES PRELIMINARY IRRADIATED WITH HIGH-INTENSE PULSED ION BEAMS

Vladislav Tarbokov[1] , Mikhail Slobodyan[2] , Sergey Pavlov[1], Egor Smolyanskiy[1], Vladimir Uglov[3] , Gennady Remnev[1]

[1]Tomsk Polytechnic University, Tomsk, 634050, Russia
[2]Tomsk Scientific Center SB RAS, Tomsk, 634055, Russia
[3]Belarusian State University, Minsk, 220030, Belarus

Attempts are currently being made to use coatings, including nitride ceramics, for improving func-tional properties of nuclear fuel claddings made of zirconium alloys. However, the incompatibility of material characteristics at the metal/ceramic interfaces, residual stresses in the coatings, as well as the morphology (roughness) of the substrate surface layers cause their low adhesion. As a result, delamina-tion often occurs during operation. This issue can be solved by optimizing the deposition parameters and preliminary treatment of the substrate surfaces by various methods. The authors report changes in adhesion of CrN coatings deposited by reactive magnetron sputtering on substrates from the Zr– 1%Nb alloy, pre-irradiated with a high-intensity pulsed ion beam (HIPIB). The effect of the HIPIB energy density on the morphology, phase composition, microhardness, and free surface energy levels of the modified layers is shown. Finally, changes in adhesion, assessed by scratch tests combined with acoustic emission signal processing, are presented. The results show that the crack initiation threshold decreases by 20% at low energy densities of up to 1 J/cm2, while it increases by 25% at 2 J/cm2.

KEY WORDS: zirconium alloy, ceramic coating, adhesion, surface modification, high-intense pulsed ion beam

1. INTRODUCTION

At present, some metals, alloys, and steels are protected with ceramic coatings for various applications (Akahoshi et al., 2020; Aouadi et al., 2020; Selvaraj et al., 2020; Attarzadeh et al., 2021; Wang et al., 2021). Attempts are being made to use nitride ones for improving functional properties of nuclear fuel claddings made of zirconium alloys (Khatkhatay et al., 2014; Lin et al., 2018; Xiao et al., 2018; Gao et al., 2019; Meng et al., 2019; Tang et al., 2019; Krejčí et al., 2020; Ham et al., 2021). However, the incompatibility of material characteristics at the metal/ ceramic interfaces (Howe et al., 1993; Liu et al., 2004; Mu et al., 2017; Guan et al., 2020; Zhao et al., 2021), residual stresses in the coatings (Lyubimov et al., 1992; Xiao et al., 2018; Mehboob et al., 2020; Muraoka and Tateno, 2020), as well as the morphology (roughness) of the surface layers of the substrate (Lin et al., 2018; Xiao et al., 2018) result in their low adhesion. This challenge can be solved by optimizing the deposition parameters (Lin et al., 2018; Xiao et al., 2018; Tang et al., 2019; Krejčí et al., 2020). Nevertheless, the issue of durability of the coatings is not limited to enhancing their quality only. An important role is also played by properties of the substrate surfaces (the morphology, chemical and phase composition), both physical and chemical interaction between the coatings and the substrates, levels, and signs of internal stresses in the coating and at the interface, the presence of a transition layer, and many others. To enhance adhesion of the coatings, various methods are used that enable achievement of several goals in a single technological cycle, such as cleaning or activating the substrate surfaces, enhancing its strength characteristics, forming a transition layer between the coatings and the

substrates or a multi-layer structure with improved adhesion between layers. These procedures include sandblasting (Giouse et al., 2019; Parchovianský et al., 2020), ultrasonic cleaning in various liquids (Parchovianský et al., 2020), chemical etching and pickling (Troia et al., 2008), as well as high-energy surface processing (Baglin, 1994; Jang et al., 2019).

From the point of view of modifying the substrate surfaces prior to coating deposition, us-ing of high-intense pulsed ion beams (HIPIB) (Remnev et al., 1999; Slobodyan et al., 2019; Tarbokov et al., 2021) is of greatest interest. Their relative heat input levels and heating rates are two orders of magnitude higher than that of electron beams with a comparable energy density. Another advantage is the fact that the irradiated surface area in one pulse can reach tens of square centimeters, in contrast to laser processing procedures. In addition, internal stresses can be varied by changing the irradiation parameters. Accordingly, an imbalance of stresses at the interface of materials with significantly different mechanical characteristics decreases. As a result, adhesion is improved when their magnitudes and signs coincide in both substrates and coatings. Unfortu-nately, few experimental data and theoretical explanations of adhesion variations have been pub-lished to date. It should be noted that adhesion depends on the chemical and phase composition of both coatings and substrates, as well as on the deposition and surface treatment parameters. There are also some gaps in knowledge about the effects of HIPIB irradiation, given the large number of possible combinations of types of coatings, metal substrates, as well as deposition methods and modes. In a recent work, Tarbokov et al. (2021) succeeded in enhancing adhesion of aluminum nitride (AlN) coatings to 321 steel substrates by preliminary HIPIB irradiation. Continuing a series of studies, the aim of this work has been to investigate CrN coatings depos-ited on the Zr–1%Nb alloy by reactive magnetron sputtering. Changes in the morphology, phase composition, microhardness, and free surface energy levels of the modified surface layers were assessed. Initially, dependences of residual stresses in trial CrN coatings on silicon substrates were estimated. Then, the CrN coatings were deposited on substrates made of the Zr–1%Nb alloy to assess their adhesion using the results of scratch tests combined with processing of acoustic emission (AE) signals. This enabled determination of the crack initiation thresholds. The depth profiles of scratches were measured by a non-contact profilometer to estimate materials wear resistance and the crack initiation thresholds.

2. MATERIALS AND METHODS

Initially, trial CrN coatings were deposited by reactive magnetron sputtering on silicon substrates with a thickness of 0.38 mm to estimate internal stresses by analogy with the articles by Mu et al. (2017) and Tarbokov et al. (2021). The magnetron power was 1 kW, the substrate temperature was 300°C, the substrate-to-target distance was 150 mm, and the partial pressure of active gases was 0.16 Pa. The variable parameters were the bias voltage (0 or 100 V) and the Ar/N_2 ratio (1:1 or 3:1), which caused different residual stresses in the trial coatings on the silicon substrates. Subsequently, the CrN coatings were deposited on the Zr–1%Nb alloy substrates (both initial and irradiated with HIPIB) using the optimal determined deposition parameters.

Polished plates 20 × 20 × 0.5 mm in size made of the Zr–1%Nb (Russian Technical Specification TU 95.166-98) alloy with a roughness Ra of about 100 nm were irradiated with the ‘TEMP-4M’ HIPIB accelerator (Tarbokov et al., 2021). The following parameters were used: an accelerating voltage of 200 kV, a pulse width at half maximum of 100 ns, and energy densities of 0.6, 1.0, 1.5, and 2.0 J/cm2. The HIPIB consisted of about 85% C+ ions and 15% protons. The ion fluences were up to 2.1 × 1014 cm–2. There were three pulses for all modes. Temperatures of

the substrate surface layers were lower than the melting points at the low-energy density levels of 0.6 and 1.0 J/cm2, while they were remelted at 1.5 and 2.0 J/cm2.

Thicknesses of the coatings were determined using an 'MII-4' microinterferometer. In the trials, mean residual stresses (σ_f) were calculated using the Stoney formula (Stoney, 1909).

Microstresses were determined by the Williamson-Hall method (Klug and Alexander, 1974) using the results of the X-ray diffraction analysis (a 'Rigaku Ultima IV' diffractometer).

The sample surfaces were investigated with a 'JEOL 6000' scanning electron microscope (SEM), while an 'NT-MDT Integra Prima' atomic force microscope was used for measuring roughness on a 100 μm length.

Vickers microhardness was determined using a 'PMT-4M' device. A load was 40 g, the indentation depth was 2.0–2.4 μm.

A 'Micro-Scratch Tester MST-S-AX-0000' facility was implemented to assess both modus of elasticity in the surface layers and adhesion of the coatings to the Zr–1%Nb alloy substrates. In the last case, the scratch tests were combined with the acoustic emission (AE) signal analysis similarly to methodologies of Xiao et al. (2018), Tang et al. (2019), Guan et al. (2020), Tarbokov et al. (2021), and Zhao et al. (2021). The diamond indenter radius was 100 μm. Depth profiles of scratches were measured by optical profilometer Micro Measure 3D Station.

Free surface energy (FSE) levels were determined using a 'CRUSS DSA25S' contact angle meter by the Owens, Wendt, Rabel, and Kaelble method within 10 minutes after HIPIB irradiation. Liquids were water and glycerin. The obtained data were processed using the 'KRÜSS ADVANCE 1.12.3.15501' software package.

3. RESULTS

3.1 Trial Coatings

Table 1 shows mean stresses in the trial CrN coatings on silicon substrates. It was concluded by analyzing these data that both stress levels and their signs could be controlled by varying the deposition parameters. For all modes, the coatings consisted of the fcc CrN phase (Fm-3m space group). The greatest CrN lattice parameters were observed with the same amount of argon and nitrogen, and the smallest ones were for their ratio of 3:1 (the bias voltage was zero for both cases). The first sample was characterized by the lowest level of microstrain of 0.495%, while the third one possessed the highest value of 1.600% (with the greatest dispersion). Thus, the second mode was chosen for deposition of the CrN coatings on the Zr–1%Nb alloy substrates, which was characterized by emerging tensile stresses.

TABLE 1: Properties of trial CrN coatings on silicon substrates depending on deposition conditions

No.	Ar/N_2 ratio	Bias voltage, V	Coating thickness, μm	Substrate bending radius, m	Mean stresses in coating, GPa (‘+’ is tensile, ‘–‘ is compressive)	Lattice parameter a, nm	Microstrains, %
1	1/1	0	2.2	–8.0	–0.3	0.418510 ± 0.000140	0.495 ± 0.017
2	3/1	0	3.1	+10.0	+0.2	0.415310 ± 0.000170	0.550 ± 0.050
3	1/1	100	2.2	–2.2	–1.1	0.418000 ± 0.000012	1.600 ± 0.600

3.2 Modified Surface Layers

Figure 1 presents SEM images of the Zr–1%Nb alloy surfaces both initial and after HIPIB irradiation at various energy densities. The microrelief of the initial surface (Fig. 1a) was characterized by contrasting grooves due to the polishing procedure. After HIPIB irradiation at both energy densities of 0.6 and 1.0 J/cm2, they were remelted only partially (Fig. 1b and 1c), while no grooves were found at the maximum investigated level of 2.0 J/cm2 (Fig. 1d). In the latter case, typical microcraters were also observed on the substrate surfaces. In this study, thicknesses of the modified layers were not measured due to high labor intensity and cost, but they were typically several micrometers for such cases (Slobodyan, 2021). After HIPIB irradiation, roughness of the modified surfaces slightly increased at the minimum studied energy density of 0.6 J/cm2, and then decreased at the remelting modes (Fig. 2). At 2.0 J/cm2, roughness values were only half of the initial levels.

Figure 3 and Table 2 show the results of X-ray diffraction analysis for both initial and HIPIB-irradiated surface layers. In the Zr–1%Nb alloy, the main phase was α-Zr, as expected

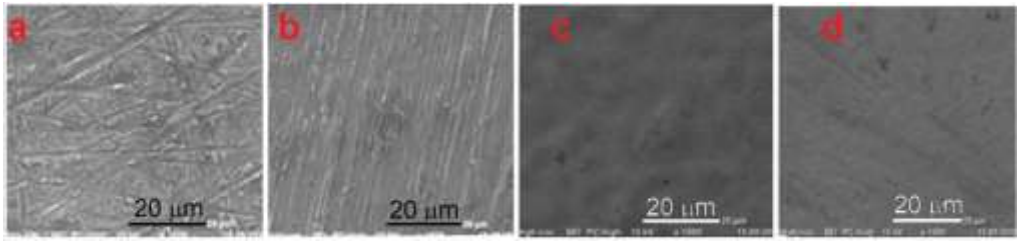

FIG. 1: The SEM-images of the Zr–1%Nb alloy surfaces: initial (a), as well as HIPIB irradiated at the energy densities of 0.6 (b), 1.0 (c), and 2.0 (d) J/cm2

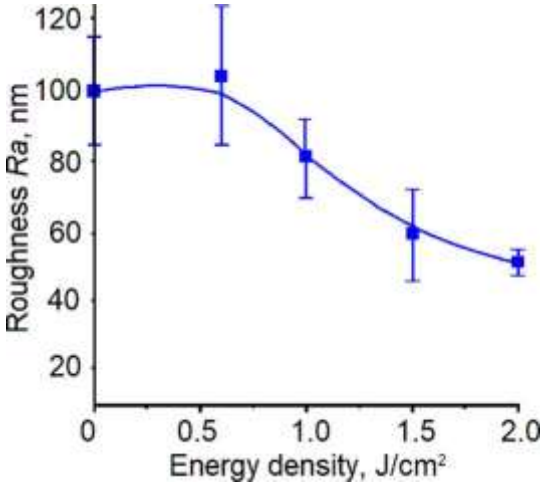

FIG. 2: The surface roughness versus HIPIB energy density

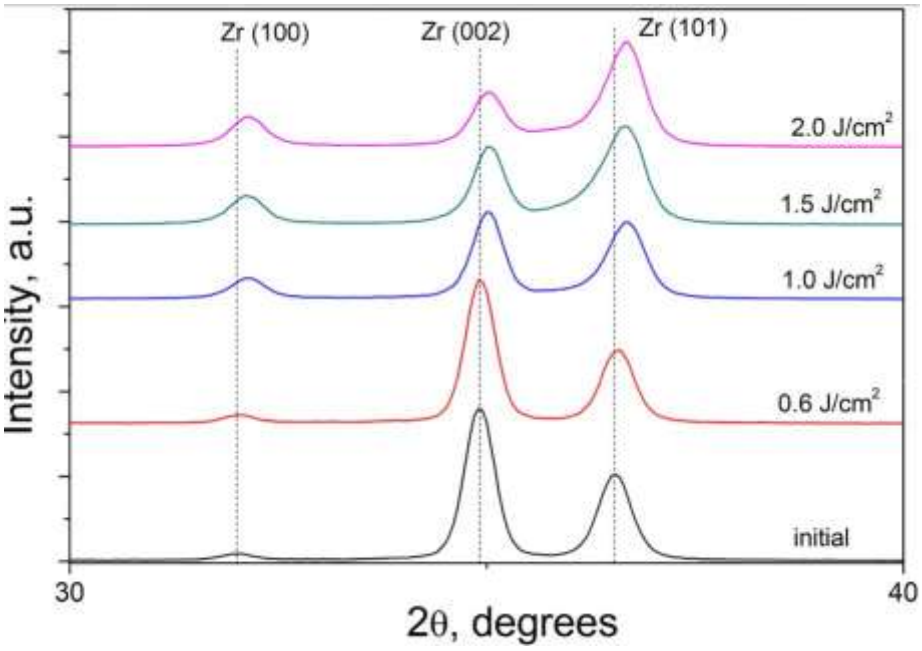

FIG. 3: The X-ray diffraction patterns of as-received samples and after HIPIB irradiation

TABLE 2: Lattice parameters and microstrains in the Zr–1%Nb alloy surface layers

HIPIB energy density, J/cm2	Lattice parameters		Microstrains, %
	a, nm	c, nm	
–	0.3239	0.5149	0.23
0.6	0.3238	0.5148	0.32
1.0	0.3227	0.5138	0.41
1.5	0.3226	0.5133	0.42
2.0	0.3226	0.5136	0.31

(Slobodyan et al., 2019; Slobodyan, 2021). Its lattice parameters exceeded those for pure zirconium (a = 0.3231 nm; c = 0.5148 nm) due to the presence of niobium as an alloying element. HIPIB irradiation did not change the phase composition of the Zr–1%Nb alloy. Both a and c lattice parameters decreased with energy density rising. Only at the maximum level of 2.0 J/cm2, the c parameter enhanced slightly. A significant increase in microstrains was observed with enhancing energy density up to 1.5 J/cm2. However, they reduced at the maximum studied value of 2.0 J/cm2.

After HIPIB irradiation, microhardness of the surface layers increased slightly at the minimum applied energy density of 0.6 J/cm2, and then decreased by 10% compared to the initial values at the maximum level of 2.0 J/cm2 (Fig. 4a). At the same time, the values of their elastic moduli showed a directly opposite relationship (Fig. 4b). The most likely reason for this phenom-enon was a decrease in the work-hardening effect of the rolled Zr–1%Nb alloy upon remelting. A significant dispersion of these values was due to its typical anisotropy and the

formation of quenched microstructures upon rapid heating and cooling, inherent in all high-energy surface treatment methods (Slobodyan, 2021).

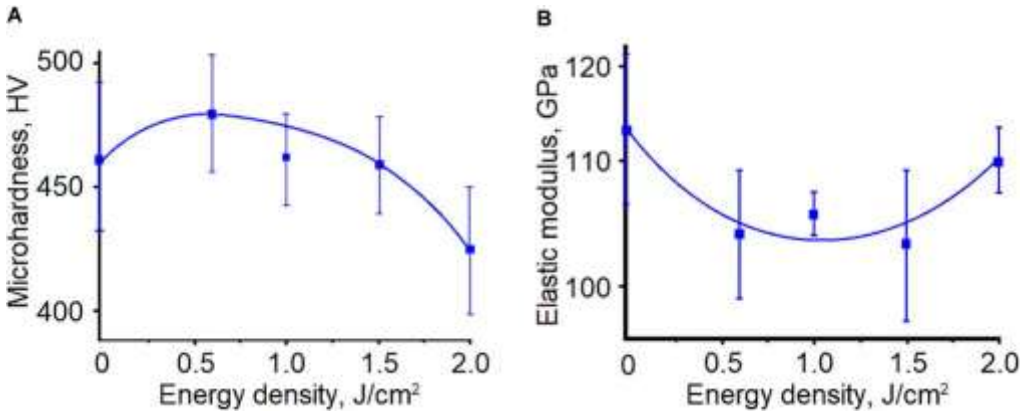

FIG. 4: Microhardness (a) and the modulus of elasticity (b) of the surface layers versus HIPIB energy density

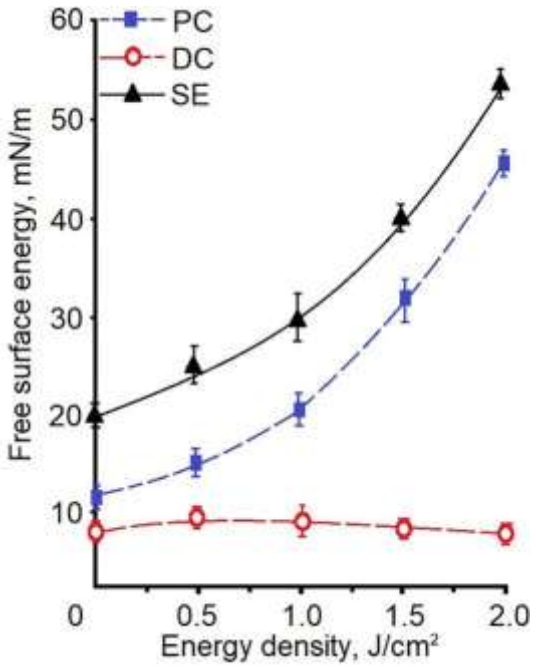

FIG. 5: The FSE levels of the surface layers versus HIPIB energy density (SE: total surface free energy; DC: dispersive component; PC: polar component)

The energy and chemical activity properties of the surface layers changed greatly after HIPIB irradiation. Both FSE and its polar component levels monotonically enhanced in the entire studied range of the HIPIB energy densities (Fig. 5), which, first of all, was connected with the

chemical activity of the surfaces. At the same time, recrystallization of the surface layer resulted in an almost complete suppression of the dispersed component, which caused reducing the levels of residual stresses at the coating/substrate interfaces. Nevertheless, a decrease in the van der Waals forces was a negative factor that effected adhesion as well.

3.3 Scratch-Test Results

Figures 6 and 7 show the results of the scratch tests. During the tests, peaks of the AE signal were associated with the initiation and propagation of cracks in the coatings due to the indenter forces (Fn) similarly to the methodologies used by Liu et al. (2004), Xiao et al. (2018), Tang et al. (2019), Guan et al. (2020), Tarbokov et al. (2021), and Zhao et al. (2021). The intensity of the AE signal peaks was proportional to the number of both formed cracks and broken interatomic bonds (the volume of the delaminated coating). For the CrN coating on the initial substrate from the Zr–1%Nb alloy, the cracking process began at an Fn value above 8.5 N. HIPIB irradiation at the energy density of 1.0 J/cm2 decreased resistance to failure of the coating, since cracks formed at a force higher than 8.5 N, while the intensity of the AE signal was greater than that of the initial substrate. Increasing the energy density up to 2.0 J/cm2 improved adhesion of the CrN coatings and shifted the crack initiation threshold to more than 14.5 N. There was not a single peak in the AE signal up to 12 N.

The results of the AE signal fixation are in accordance with the profilometry data. Figure 7 shows the dependence of the scratch depth on the magnitude of the applied load. Taking into account that the samples were tested at the same rate of the load increase, the value of the ultimate load and the path length, it can be argued that a larger scratch depth corresponds to a lower wear resistance. It can be seen that the coating deposited on the substrate preliminarily irradiated with an energy density of 2 J/cm2 has the highest wear resistance. The onset of active destruction in this case is in the range of 13.5–14.5 N. For the original sample, this value is 12.5 N, and for the sample irradiated with an energy density of 1 J/cm2, it is 9 N. However, the behavior of coatings deposited on different substrates differs at a load value preceding the onset of active destruction. Thus, a coating deposited on a substrate treated with an energy density of 2 J/cm2 is practically not subject to wear at a load of up to 8 N, and the scratch depth at 11 N is about 1 μm. In contrast, a coating deposited on a substrate without treatment and treated with 1 J/cm2 does not have such protective properties. The scratch depth begins to increase immediately with increasing load and at the moment preceding the onset of active destruction is 5.5 μm and 8 μm, respectively.

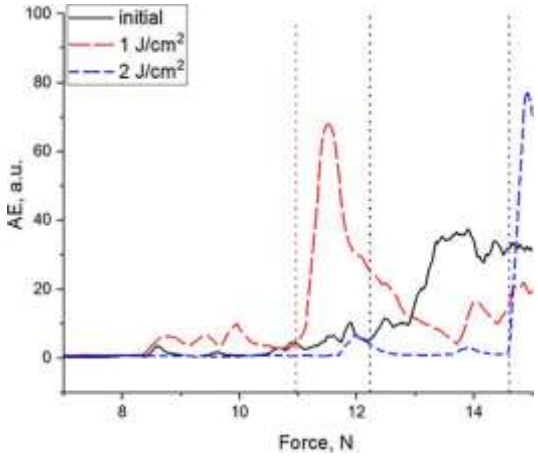

FIG. 6: The results of the scratch tests of the CrN coatings on the Zr–1%Nb alloy substrates

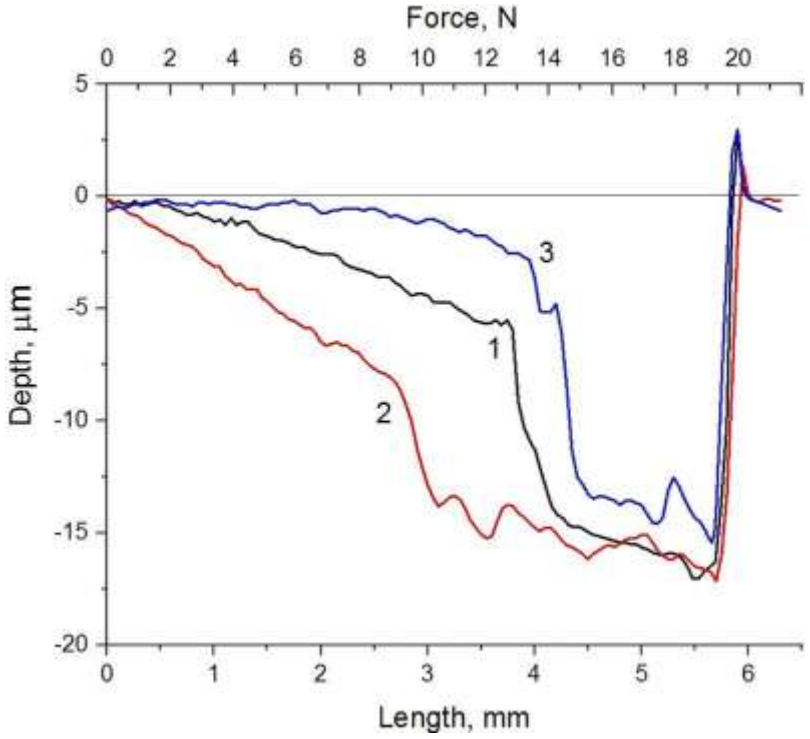

FIG. 7: The depth profiles of scratches for CrN coatings deposited on Zr–1%Nb substrates irradiated by HIPIB with different energy densities: 1: non-irradiated; 2: 1 J/cm2; 3: 2 J/cm2

4. DISCUSSION

Adhesion at the ceramic/metal interfaces was affected by many factors, such as the morphology (roughness) and chemical composition of the surface layers, their microstructure, plastic and elastic properties of both coating and substrate materials, residual internal stresses, the presence of defects and their sizes, as well as loading conditions (Martin, 2010; Xiao et al., 2018; Tang et al., 2019; Tarbokov et al., 2021). Considering that HIPIB irradiation changed many of them in the surface layers of the Zr–1%Nb alloy (at least the morphology, phase composition, micro-hardness, and FSE levels), each contribution to the variation of the scratch test results had to be considered.

As for the effect of roughness of metal substrates on adhesion of ceramic coatings, few comparable data were published to date. The closest results were obtained for TiN coatings deposited on Zircaloy-4 substrates by magnetron sputtering (Xiao et al., 2018). Adhesion lev-els were also determined by scratch tests. Xiao et al. (2018) showed that roughness of the substrate surfaces significantly affected the microstructure and residual stresses in the coat-ings, as well as their adhesion (all these parameters did not change monotonically). The bond strength tended to first increase and then decrease with rising substrate surface roughness. The results obtained in this study confirmed the tendency by the example of the CrN coatings on the substrates made of the Zr–1%Nb alloy. The dependence of the changes in roughness on the modified surface layers on the HIPIB energy density (Fig. 2) correlated with the dynam-ics of the crack initiation thresholds during the scratch test (Fig. 6) . Most likely, the reason was that HIPIB irradiation cleared the substrate surfaces from most contaminants and broke chains of the surface bonds, exposing the active centers on which the deposited coatings were covalently bonded (Baglin, 1994). The increase in the substrate roughness in combination with HIPIB irradiation activated the reactivity of the metal/ceramic interface and caused extremely effective adhesion. This fact was also confirmed in the obtained results, as follows from the comparison of FSE levels (Fig. 5) and the scratch test results (Fig. 6). It should be noted that ion irradiation caused the formation of rough surfaces on some inhomogeneous substrates (Ba-glin, 1994), which strengthened the interface formed due to its fracture toughness, as well as the increased area of a clean contact. At the same time, preliminary plasma treatment enabled ceramic surfaces made of aluminum, copper, and AlN to possess hydrophilic properties due to the removal of oxides and impurities, which could increase the reactivity of the surface (Jang et al., 2019). The bond strength of AlN coatings on both aluminum and copper substrates en-hanced with an increase in both plasma power and treatment duration. However, adhesion at the porcelain/titanium interface was improved by preliminary sandblasting and surface treat-ment with electric discharge (Troia et al., 2008) . The aforementioned set of conflicting results led to the conclusion that high-energy surface processing can improve adhesion of ceramic coatings and metal substrates only when the optimal methods and parameters were applied for each particular combination.

In continuation of the study by Xiao et al. (2018), the effect of bias stress on adhesion and residual stresses in TiN coatings on Zircaloy-4 substrates was shown by the same authors in Tang et al. (2019). The adhesion also did not change monotonically with an increase in the negative bias on the substrates (the TiN coating deposited at a voltage of –100 V withstands the maximum critical load). The TiN coatings were characterized by residual compressive stresses, which were higher after deposition at –200 and –300 V than those obtained at –50 and –100 V. Tensile tests showed no obvious difference between the strength characteristics of the samples.

In the present study, the bias voltage did not have a positive effect on optimization of residual stresses in the trial CrN coatings on the silicon substrates. Therefore, this technological method was not applied when depositing them on the Zr–1%Nb alloy. However, it was possible that this parameter can also contribute to an increase in adhesion, since two types of residual

stresses could be formed in the coatings (Martin, 2010). The former enhanced due to inhomogeneities arising upon the deposition process, but the second type increased because of a mismatch be-tween the thermal expansion coefficients of the substrates and the coatings. These levels were determined by both substrate dimensions and the ratio of the thermal expansion coefficients. Since these characteristics were different for the Zr–1%Nb alloy and the silicon substrates, the residual stresses were also different. Accordingly, more research is needed to confirm or disprove this hypothesis.

The mechanical properties of the modified surface layers also varied with the increase in the HIPIB energy density (Fig. 4). This result could have a double effect on adhesion of the CrN coatings. For example, cracks usually propagated in ceramics adjacent to substrates towards the base metals (including through their interfaces) in cases of poor adhesion, while they transformed into a brittle intermediate layer for coatings with good bonding (Howe, 1993). As another exam-ple, studies of Cr_3C_2-NiCr coatings deposited on pre-sandblasted 17-4PH steel substrates showed ambiguous results (Giouse et al., 2019). On the one hand, a positive effect on adhesion was ob-served due to a change in roughness. However, the microstructure and mechanical properties also changed in the surface layer (at the interface, hardness increased by more than 20% compared to that in the bulk metal). In addition, residual alumina particles were a reason of the formation of cracks that initiated at their edges and caused fracture through the surface layer. Similar results were obtained for glass–ceramic coatings deposited on 441 stainless steel substrates after pre-liminary sandblasting (Parchovianský et al., 2020).

Finally, it should be noted that the obtained results were considered as primary. They require additional experimental and theoretical substantiation. For a more accurate study of both me-chanical and tribological characteristics, it is necessary to apply more research methods. This is the goal of further research by the authors.

5. CONCLUSIONS

The following conclusions were drawn based on the obtained results:

1. HIPIB irradiation caused the change in the surface morphology of the Zr–1%Nb alloy.
   In the initial state, it was characterized by clearly distinguishable grinding grooves, which were partially remelted at energy densities of 0.6 and 1.0 J/cm2 and completely recrystallized at 2.0 J/cm2. Roughness of the modified surfaces slightly increased at the minimum energy density of 0.6 J/cm2, and then decreased down to a half of the initial values at 2.0 J/cm2.
2. Microhardness of the surface layers enhanced slightly at the minimum used energy density of 0.6 J/cm2, and then decreased by 10% compared to the initial value at the maximum level of 2.0 J/cm2. At the same time, their values of the modulus of elasticity showed a directly opposite relationship. The most likely reason for this phenomenon was a decrease in the work-hardening effect of the rolled Zr–1%Nb alloy upon remelt-ing. A significant dispersion of these values was explained by its typical anisotropy and the formation of quenched microstructures upon rapid heating and cooling, inherent in all high-energy surface treatment methods.
3. After HIPIB irradiation, the energy and chemical activity properties changed greatly in the surface layers. Over the entire studied range of energy densities, the FSE levels monotonically increased, and their polar component also reached its maximum level.
   This fact, among other things, reflected the chemical activity of the surfaces. At the same time, recrystallization of the surface layer caused almost complete suppression of the dispersed component. On the one hand, this could have a positive effect on reducing the levels of residual

stresses at the coating/substrate interfaces. However, a negative effect on adhesion was also possible due to a decrease in the van der Waals forces.

4. The scratch tests combined with AE signal processing showed that the cracking pro-cess started at the force greater than 8.5 N and ended at the pressure greater than 13 N for the CrN coating on the initial Zr–1% Nb alloy substrate. HIPIB irradiation of the substrate at the energy density of 1.0 J/cm2 decreased the fracture resistance of the coating: cracks were formed at the force higher than 8.5 N, and the AE signal intensity was greater than that for the initial substrate. Raising the energy density up to 2.0 J/ cm2 improved adhesion of the coating and shifted the crack initiation threshold to more than 14.5 N. Even a single peak of the AE signal was absent to 12 N. According to the authors, the improvement in adhesion was associated with the decrease in roughness of the modified surface and optimization of a set of the mechanical properties and the free surface energy levels.

ACKNOWLEDGEMENTS

This research was funded by RFBR and ROSATOM (Grant No. 20-21-00025).

REFERENCES

Akahoshi, E., Matsunaga, M., Kimura, K., Nakamura, K., Balden, M., Hishinuma, Y., and Chikada, T., Cor-rosion Tests of Multi-Layer Ceramic Coatings in Liquid Lithium-Lead, Fusion Eng. Des., vol. 160, p. 111874, 2020. DOI: 10.1016/j.fusengdes.2020.111874

Aouadi, S.M., Gu, J., and Berman, D., Self-Healing Ceramic Coatings that Operate in Extreme Environ-ments: A Review, J. Vac. Sci. Technol., vol. 38, no. 5, p. 050802, 2020. DOI: 10.1116/6.0000350 Attarzadeh, N., Molaei, M., Babaei, K., and Fattah-alhosseini, A., New Promising Ceramic Coatings for Corrosion and Wear Protection of Steels: A Review, Surf. Interfaces, vol. 23, p. 100997, 2021. DOI: 10.1016/j.surfin.2021.100997

Baglin, J.E.E., Thin Film Bonding Using Ion Beam Techniques – A Review, IBM J. Res. Dev., vol. 38, no. 4, pp. 413–422, 1994. DOI: 10.1147/rd.384.0413

Gao, Z., Kulczyk-Malecka, J., Bousser, E., Zhang, X., Chen, Y., Liu, H., Kelly, P., and Xiao, P., Sputter-Deposited Nitrides for Oxidation Protection in a Steam Environment at High Temperatures, Thin Solid Films, vol. 688, p. 137439, 2019. DOI: 10.1016/j.tsf.2019.137439

Giouse, J.-B., White, K., and Tromas, C., Nanoindentation Characterization of the Surface Mechanical Properties of a 17-4PH Stainless Steel Substrate Treated with Grit Blasting and Coated with a Cr3C2-NiCr Coating, Surf. Coat. Technol., vol. 368, pp. 119–125, 2019. DOI: 10.1016/j.surfcoat.2019.01.050 Guan, X., Wang, Y., and Xue, Q., Effects of Constituent Layers and Interfaces on the Mechanical and Tribo-logical Properties of Metal (Cr, Zr)/Ceramic (CrN, ZrN) Multilayer Systems, Appl. Surf. Sci., vol. 502, p. 144305, 2020. DOI: 10.1016/j.apsusc.2019.144305

Ham, J., Lee, Y., Yoo, S.C., Short, M.P., Bahn, C.B., and Kim, J.H., Effect of TiN Coating on the Fouling Behavior of Crud on Pressurized Water Reactor Fuel Cladding, J. Nucl. Mater., vol. 549, p. 152870, 2021. DOI: 10.1016/j.jnucmat.2021.152870

Hopcroft, M.A., Nix, W.D., and Kenny, T.W., What is the Young's Modulus of Silicon? J. Microelectro-mech. Syst., vol. 19, no. 2, pp. 229–238, 2010. DOI: 10.1109/JMEMS.2009.2039697

Howe, J.M., Bonding, Structure, and Properties of Metal/Ceramic Interfaces. Part 2. Interface Fracture Be-haviour and Property Measurement, Int. Mater. Rev., vol. 38, no. 5, pp. 257–271, 1993. DOI: 10.1179/ imr.1993.38.5.257

Jang, K.-B., Mhin, S., Lim, S.-C., Song, Y.-S., Lee, K.-H., Park, S.-K., Moon, K.-I., Lee, S.H., and Hyun, S.-K., Room Temperature Bonding on Interface between Metal and Ceramic, J. Electron. Mater., vol. 48, no. 1, pp. 72–78, 2019. DOI: 10.1007/s11664-018-6693-8
Khatkhatay, F., Jiao, L., Jian, J., Zhang, W., Jiao, Z., Gan, J., Zhang, H., Zhang, X., and Wang, H., Superior Corrosion Resistance Properties of TiN-Based Coatings on Zircaloy Tubes in Supercritical Water, J. Nucl. Mater., vol. 451, pp. 346–351, 2014. DOI: 10.1016/j.jnucmat.2014.04.010
Klug, H.P. and Alexander, L.E., X-Ray Diffraction Procedures, Hoboken, NJ: John Wiley & Sons Inc., 1974.
Krejčí, J., Kabátová, J., Manoch, F., Kočí, J., Cvrček, L., Málek, J., Krum, S., Šutta, P., Bublíková, P., Hal-odová, P., Namburi, H.K., and Ševeček, M., Development and Testing of Multicomponent Fuel Clad-ding with Enhanced Accidental Performance, Nucl. Eng. Technol., vol. 52, no. 3, pp. 597–609, 2020. DOI: 10.1016/j.net.2019.08.015
Lin, S., Zhang, J., Zhu, R., Fu, S., and Yun, D., Effects of Sputtering Pressure on Microstructure and Me-chanical Properties of ZrN Films Deposited by Magnetron Sputtering, Mater. Res. Bull., vol. 105, pp. 231–236, 2018. DOI: 10.1016/j.materresbull.2018.04.054
Liu, L.M., Wang, S.Q., and Ye, H.Q., Atomic and Electronic Structures of the Lattice Mismatched Metal-Ce-ramic Interface, J. Condens. Matter Phys., vol. 16, no. 32, pp. 5781–5790, 2004. DOI: 10.1088/0953-8984/16/32/014
Lyubimov, V.V., Voevodin, A.A., Spassky, S.E., and Yerokhin, A.L., Stress Analysis and Failure Possibility Assessment of Multilayer Physically Vapour Deposited Coatings, Thin Solid Films, vol. 207, nos. 1–2, pp. 117–125, 1992. DOI: 10.1016/0040-6090(92)90111-N
Martin, P.M., Handbook Deposition Technologies for Film Coatings, Oxford, UK: Elsevier, 2010.
Mehboob, G., Liu, M.-J., Xu, T., Hussain, S., Mehboob, G., and Tahir, A., A Review on Failure Mechanism of Thermal Barrier Coatings and Strategies to Extend Their Lifetime, Ceram. Int., vol. 46, no. 7, pp. 8497–8521, 2020. DOI: 10.1016/j.ceramint.2019.12.200
Meng, C., Yang, L., Wu, Y., Tan, J., Dang, W., He, X., and Ma, X., Study of the Oxidation Behavior of CrN Coating on Zr Alloy in Air, J. Nucl. Mater., vol. 515, pp. 354–369, 2019. DOI: 10.1016/j.jnuc-mat.2019.01.006
Mu, Y., Zhang, X., Hutchinson, J.W., and Meng, W.J., Measuring Critical Stress for Shear Failure of In-terfacial Regions in Coating/Interlayer/Substrate Systems through a Micro-Pillar Testing Protocol, J. Mater. Res., vol. 32, no. 8, pp. 1421–1431, 2017. DOI: 10.1557/jmr.2016.516
Muraoka, S. and Tateno, M., Dependence of Bonding Strength and Variations in Residual Stress on Inter-face Wedge Angles and Bonding Temperature Conditions, MRS Adv., vol. 5, pp. 1765–1774, 2020. DOI: 10.1557/adv.2020.156
Parchovianský, M., Parchovianská, I., Švančárek, P., Motz, G., and Galusek, D., PDC Glass/Ceramic Coat-ings Applied to Differently Pretreated AISI441 Stainless Steel Substrates, Materials, vol. 13, no. 3, p. 629, 2020. DOI: 10.3390/ma13030629
Remnev, G.E., Isakov, I.F., Opekounov, M.S., Matvienko, V.M., Ryzhkov, V.A., Struts, V.K., Grushin, I.I., Zakoutayev, A.N., Potyomkin, A.V., Tarbokov, V.A., Pushkaryov, A.N., Kutuzov, V.L., and Ovsyan-nikov, M.Yu., High Intensity Pulsed Ion Beam Sources and Their Industrial Applications, Surf. Coat. Technol., vol. 114, pp. 206–212, 1999. DOI: 10.1016/S0257-8972(99)00058-4
Russian Technical Specification TU 95.166-98n Zirconium Alloys in Ingots (in Russian).
Selvaraj, S.K., Srinivasan, K., Deshmukh, J., Agrawal, D., Mungilwar, S., Jagtap, R., and Hu, Y.-C., Per-formance Comparison of Advanced Ceramic Cladding Approaches via Solid-State and

Traditional Welding Processes: A Review, Materials, vol. 13, no. 24, p. 5805, 2020. DOI: 10.3390/ma13245805
Slobodyan, M., High-Energy Surface Processing of Zirconium Alloys for Fuel Claddings of Water-Cooled Nuclear Reactors, Nucl. Eng. Des., vol. 382, p. 111364, 2021. DOI: 10.1016/j.nucengdes.2021.111364 Slobodyan, M.S., Pavlov, S.K., and Remnev, G.E., Corrosion and High-Temperature Steam Oxidation of
E110 Alloy and Its Laser Welds after Ion Irradiation, Corros. Sci., vol. 152, pp. 60–74, 2019.
Stoney, G.G., The Tension of Metallic Films Deposited by Electrolysis, Proc. R. Soc. A, vol. 82, pp. 172– 175, 1909. DOI: 10.1016/j.corsci.2019.02.031
Tang, D., Chen, H., Xiao, W., Deng, H., Zou, S., Ren, Y., Lei, M., and Zhou, X., Substrate Bias Effects on Mechanical Properties and High Temperature Oxidation Performance of Sputtered TiN-Coated Zr-4, J. Nucl. Mater., vol. 524, pp. 330–339, 2019. DOI: 10.1016/j.jnucmat.2019.07.013
Tarbokov, V., Pavlov S., Smolyanskiy, E., Uglov, V., Slobodyan, M., and Remnev, G., Effect of Preliminary Irradiation of 321 Steel Substrates with High-Intense Pulsed Ion Beams on Scratch Test Results of Subsequently Deposited AlN Coatings, Coatings, vol. 11, no. 10 p. 1169, 2021. DOI: 10.3390/coat-ings11101169
Troia, M.G., Jr., Henriques, G.E.P., Mesquita, M.F., and Fragoso, W.S., The Effect of Surface Modifications on Titanium to Enable Titanium-Porcelain Bonding, Dent. Mater., vol. 24, no. 1, pp. 28–33, 2008. DOI: 10.1016/j.dental.2007.01.009
Wang, H., Xiao, J., Wang, H., Chen, Y., Yin, X., and Guo, N., Corrosion Behavior and Surface Treatment of Cladding Materials Used in High-Temperature Lead-Bismuth Eutectic Alloy: A Review, Coatings, vol. 11, no. 3, p. 364, 2021. DOI: 10.3390/coatings11030364
Xiao, W., Deng, H., Zou, S., Ren, Y., Tang, D., Lei, M., Xiao, C., Zhou, X., and Chen, Y., Effect of Rough-ness of Substrate and Sputtering Power on the Properties of TiN Coatings Deposited by Magnetron Sputtering for ATF, J. Nucl. Mater., vol. 509, pp. 542–549, 2018. DOI: 10.1016/j.jnucmat.2018.07.011 Zhao, Z., Liu, F., Cao, L., Du, Y., Li, B., Li, J., and Xu, Y., Investigation of Indentation Response, Scratch Resistance, and Wear Behavior of Tungsten Carbide Coatings Fabricated by Two-Step Interstitial Car-burization on Tungsten, Ceram. Int., vol. 47, no. 21, pp. 30636–30647, 2021. DOI: 10.1016/j.cera-
mint.2021.07.241